

Article

Proteomic Profiling of Iron Overload-Induced Human Hepatic Cells Reveals Activation of TLR2-Mediated Inflammatory Response

Xiang Li ^{1,*}, Shiwei Li ^{2,3,†}, Mize Lu ⁴, Guohua Yang ⁴, Yunfeng Shen ⁴ and Xin Zhou ^{4,*}

¹ Wuxi Medical School, Jiangnan University, Wuxi 214122, China

² Key Laboratory of Carbohydrate Chemistry & Biotechnology Ministry of Education, Jiangnan University, Wuxi 214122, China; shiweili099@sohu.com

³ School of Biotechnology, Jiangnan University, Wuxi 214122, China

⁴ Department of Hematology, Wuxi People's Hospital, Wuxi 214023, China; lmzmedsci@163.com (M.L.); wxygh@medmail.com.cn (G.Y.); yfshen21cn2012@hotmail.com (Y.S.)

* Correspondence: xiangli@jiangnan.edu.cn (X.L.); 13358111962@189.cn (X.Z.); Tel./Fax: +86-510-8591-8126 (X.L.); Tel.: +86-510-8535-0202 (X.Z.)

† These authors contributed equally to this work.

Academic Editor: Norbert Latruffe

Received: 25 January 2016 ; Accepted: 2 March 2016 ; Published: 17 March 2016

Abstract: Background: Hepatic iron overload is common in patients who have undergone hematopoietic cell transplantation (HCT) and may predispose to peri- and post-HCT toxicity. To better reveal more molecules that might be involved in iron overload-induced liver injury, we utilized proteomics to investigate differentially expressed proteins in iron overload-induced hepatocytes *vs.* untreated hepatocytes. Methods and Results: HH4 hepatocytes were exposed to ferric ammonium citrate (FAC) to establish an *in vitro* iron overload model. Differentially expressed proteins initiated by the iron overload were studied by two-dimensional liquid chromatography tandem mass spectrometry (2D-LC-MS) analysis. We identified 93 proteins whose quantity statistically significantly changes under excess hepatocyte iron conditions. Gene Ontology (GO) analysis showed that these differentially expressed proteins in HH4 cells are involved in various biological process including endocytosis, response to wounding, di-, trivalent inorganic cation homeostasis, inflammatory response, positive regulation of cytokine production, and *etc.* Meanwhile, proteomics data revealed protein level of TLR2 and IL6ST significantly increased 7 times and 2.9 times, respectively, in iron overloaded HH4 cells. Our subsequent experiments detected that FAC-treated HH4 cells can activate IL6 expression through TLR2-mediated inflammatory responses via the NF- κ B pathway. Conclusions: In this study, we demonstrated that iron overload induced hepatocytes triggering TLR2-mediated inflammatory response via NF- κ B signaling pathway in HH4 cells.

Keywords: iron overload; proteomics; TLR2; IL-6; NF- κ B

1. Introduction

Allogeneic hematopoietic cell transplantation (HCT) has been developed to cure clonal disorder diseases, such as myelodysplastic syndromes (MDS) [1,2]. Preclinical and limited clinical data suggest that iron overload related to anemia, red blood cell transfusions and, possibly other factors, may be associated with hepatic injury in patients undergoing HCT [1,3]. Iron overload will lead to tissue damage and even iron poisoning because cells lack an effective way to dispose of the excessive iron. The liver is the major organ for iron storage and patients with chronic iron overload in the liver are at significantly higher risk of further developing liver fibrosis, cirrhosis, and hepatocellular carcinoma [4].

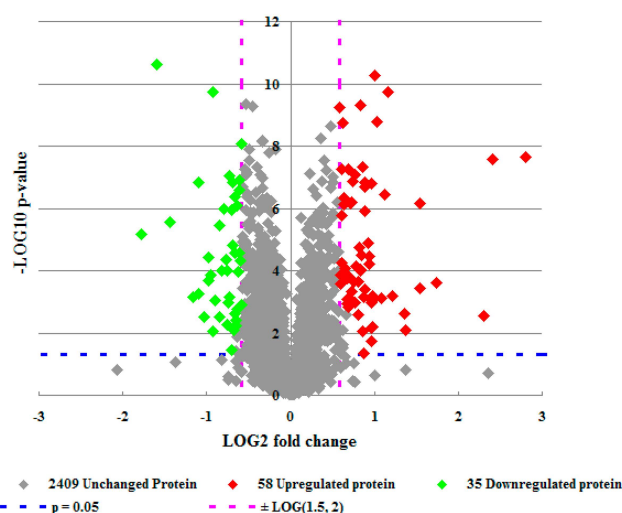
Our previous work have shown that ferric ammonium citrate (FAC)-induced iron overload in HH4 cells was capable of increasing apoptosis through an iron-generated ROS-activated signaling pathway [5], however the cellular consequences and process of iron overload in hepatocytes are still not very clear and need to be further elucidated. Therefore, the current study was aimed at assessing protein expression changes initiated by excess iron using a proteomic approach. We attempted to characterize the new “molecules” that are involved in inflammatory response induced by iron overload in HH4 cells. Our proteomics data revealed protein levels of Toll-like receptor 2 (TLR2) and IL6ST significantly increased seven times and 2.9 times, respectively, in iron overload HH4 cells. The subsequent results detected that FAC-treated HH4 cells can activate IL6 expression through TLR2-mediated inflammatory responses via NF- κ B signaling pathway in HH4 cells.

2. Results

2.1. Overview of Proteomic Analysis (2D-LC-MS)

To gain insight into the effect of FAC-induced iron overload on HH4 cells, 2D-LC-MS were carried out to compare the protein profiles of HH4 cells stimulated by FAC at concentrations of 0 and 5 mM, respectively. A total of 2502 unique proteins were identified in both of the two independent replicate experiments. Among these, expression of 58 proteins was higher (more than 1.5-fold) and expression of 35 proteins was lower (less than 0.67 fold) in FAC-treatment HH4 cells compared to untreated cells (Figure 1A and Table 1). Next, we analyzed the main properties of these identified differentially expressed proteins using the Database for Annotation, Visualization and Integrated Discovery (DAVID) gene bioinformatic resources. The results showed these differentially expressed proteins are involved in various biological process mainly including response to wounding, di-, tri-valent inorganic cation homeostasis, regulation of growth, positive regulation of signal transduction, anti-apoptosis, inflammatory response, *etc.* (Figure 1B and Table 2).

In addition, Gene Ontology (GO) analysis revealed that the most common molecular functions were purine nucleotide binding, ribonucleotide binding, adenyly nucleotide binding and identical protein binding (Figure 1C). On the other hand, the major cellular component categories were membrane-enclosed lumen, mitochondrion, golgi apparatus, endoplasmic reticulum and cell surface (Figure 1D). Subsequently, on the basis of KEGG pathways, we found that highly significant enrichment was seen in several pathways mainly including lysosome, hematopoietic cell lineage and drug metabolism (Figure 1E).



(A)

Figure 1. Cont.

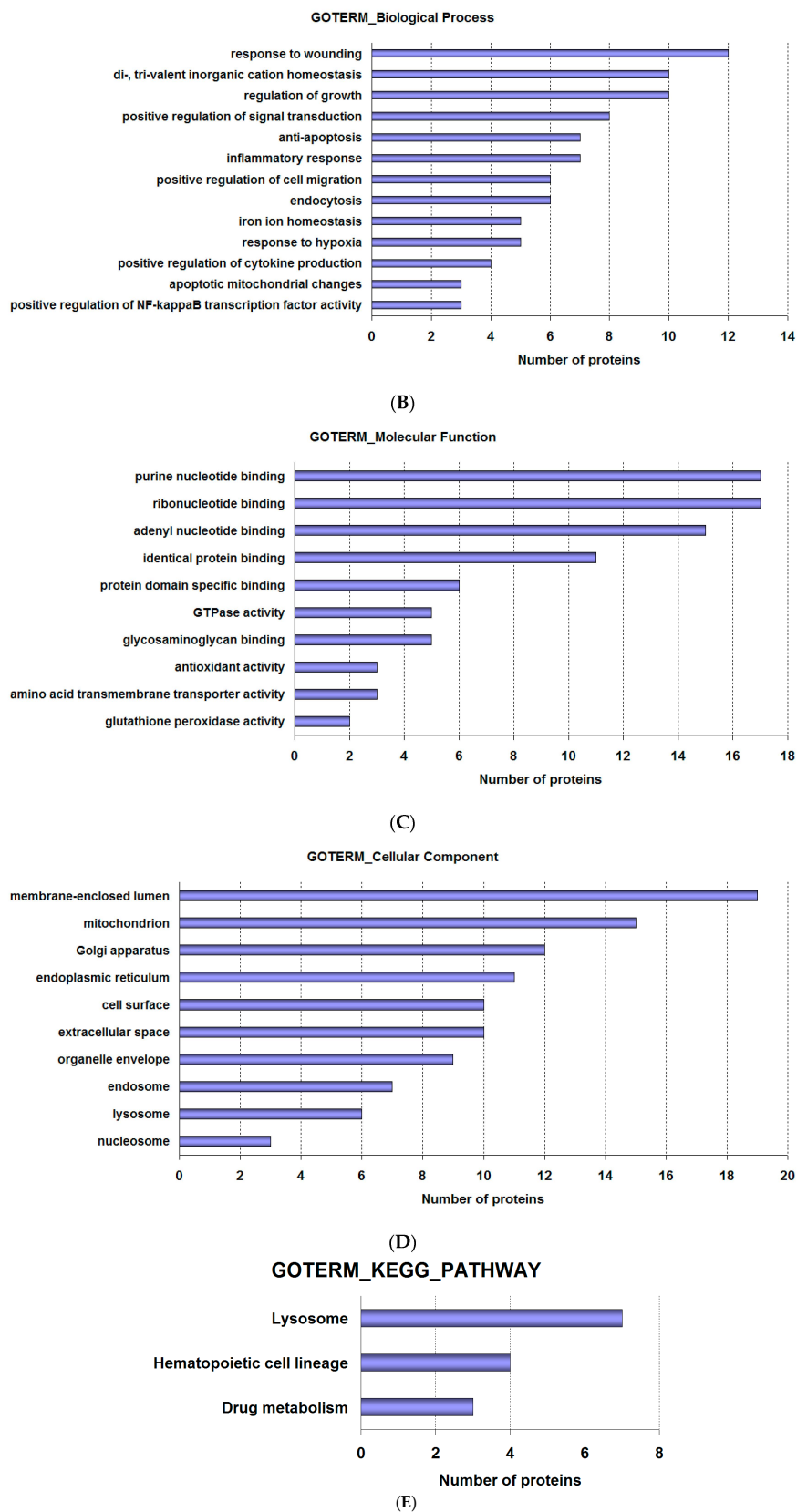


Figure 1. Differential proteomic analysis in HH4 cells. (A) Volcano plot of 2502 differentially expressed proteins between iron overload treatment group and control group in HH4 cells. (B–D) Functional classification of differentially expressed proteins using SWISS-PROT database based on universal GO annotation terms. Proteins shown were linked to at least one annotation term within the GO biological process (B); molecular function (C); and cellular component (D) categories; (E) KEGG pathway analysis.

Table 1. Proteins differentially expressed in response to iron overload in HH4 cells.

| Ratio ¹ | Protein IDs | Protein Description | Gene Name | MW [kDa] ² |
|--------------------|-------------|--|-----------|-----------------------|
| −1.781 | Q92896 | Golgi apparatus protein 1 | GLG1 | 135 |
| −1.602 | Q9NZN4 | EH domain-containing protein 2 | EHD2 | 61 |
| −1.437 | P09972 | Fructose-bisphosphate aldolase C | ALDOC | 39 |
| −1.091 | P42126 | Isoform 2 of Enoyl-CoA delta isomerase 1, mitochondrial | ECI1 | 31 |
| −1.09 | P07996 | Thrombospondin-1 | THBS1 | 129 |
| −0.983 | P09603 | Macrophage colony-stimulating factor 1 | CSF1 | 60 |
| −0.977 | Q92522 | Histone H1x | H1FX | 22 |
| −0.956 | O95197 | Isoform 3 of Reticulon-3 | RTN3 | 26 |
| −0.927 | P21399 | Cytoplasmic aconitate hydratase | ACO1 | 98 |
| −0.895 | Q15418 | Isoform 3 of Ribosomal protein S6 kinase α -1 | RPS6KA1 | 73 |
| −0.845 | P07203 | Glutathione peroxidase 1 | GPX1 | 22 |
| −0.814 | Q8TED1 | Probable glutathione peroxidase 8 | GPX8 | 24 |
| −0.793 | Q16678 | Cytochrome P450 1B1 | CYP1B1 | 61 |
| −0.768 | Q6EMK4 | Vasorin | VASN | 72 |
| −0.749 | P51580 | Thiopurine S-methyltransferase | TPMT | 28 |
| −0.745 | Q969V3 | Isoform 2 of Nicalin | NCLN | 63 |
| −0.733 | O00622 | Protein CYR61 | CYR61 | 42 |
| −0.729 | P06865 | β -Hexosaminidase | HEXA | 58 |
| −0.7 | P04179 | Superoxide dismutase [Mn], mitochondrial | SOD2 | 25 |
| −0.693 | P17342 | Isoform 2 of atrial natriuretic peptide receptor 3 | NPR3 | 60 |
| −0.685 | P07602 | Proactivator polypeptide | PSAP | 58 |
| −0.661 | O43865 | Putative adenosylhomocysteinase 2 | AHCYL1 | 59 |
| −0.657 | P52630 | Signal transducer and activator of transcription 2 | STAT2 | 97 |
| −0.657 | P51553 | Isocitrate dehydrogenase [NAD] subunit gamma, mitochondrial | IDH3G | 43 |
| −0.648 | P61970 | Nuclear transport factor 2 | NUTF2 | 14 |
| −0.647 | Q9ULZ3 | Apoptosis-associated speck-like protein containing a CARD (PYD and CARD domain containing) | PYCARD | 22 |
| −0.639 | P30626 | Sorcin | SRI | 18 |
| −0.637 | P0DMM9 | Sulfotransferase 1A3 | SULT1A3 | 34 |
| −0.617 | Q9H845 | Acyl-CoA dehydrogenase family member 9, mitochondrial | ACAD9 | 69 |
| −0.615 | P53634 | Dipeptidyl peptidase 1 | CTSC | 52 |
| −0.613 | Q6P587 | Acylpyruvase FAHD1, mitochondrial | FAHD1 | 25 |
| −0.609 | P16403 | Histone H1.2 | HIST1H1C | 21 |
| −0.602 | P62805 | Histone H4 | HIST1H4A | 11 |
| −0.59 | P04844 | Isoform 2 of Dolichyl-diphosphooligosaccharide—protein glycosyltransferase subunit 2 | RPN2 | 68 |
| −0.588 | Q13228 | Selenium-binding protein 1 | SELENBP1 | 52 |
| 0.586 | P05362 | Intercellular adhesion molecule 1 | ICAM1 | 58 |
| 0.597 | Q9Y6H1 | Coiled-coil-helix-coiled-coil-helix domain-containing protein 2, mitochondrial | CHCHD2 | 16 |
| 0.601 | Q9Y371 | Endophilin-B1 | SH3GLB1 | 41 |
| 0.61 | P05161 | Ubiquitin-like protein ISG15 | ISG15 | 18 |
| 0.614 | P31689 | DnaJ homolog subfamily A member 1 | DNAAJ1 | 45 |
| 0.614 | P11387 | DNA topoisomerase 1 | TOP1 | 91 |
| 0.621 | P31153 | S-adenosylmethionine synthase isoform type-2 | MAT2A | 44 |
| 0.636 | Q14498 | Isoform 3 of RNA-binding protein 39 | RBM39 | 57 |
| 0.636 | O75534 | Isoform Short of Cold shock domain-containing protein E1 | CSDE1 | 86 |
| 0.643 | P02786 | Transferrin receptor protein 1 | TfR1 | 85 |
| 0.653 | Q75976 | Carboxypeptidase D | CPD | 153 |
| 0.656 | Q9BQ52 | Zinc phosphodiesterase ELAC protein 2 | ELAC2 | 92 |
| 0.67 | Q9UI12 | ATPase, H ⁺ transporting, lysosomal 50/57kDa, V1 subunit H, isoform CRA_c | ATP6V1H | 52 |
| 0.678 | P48729 | Casein kinase 1, alpha 1, isoform CRA_g | CSNK1A1 | 38 |
| 0.681 | P08473 | Neprilysin | MME | 86 |
| 0.685 | Q9H2H9 | Sodium-coupled neutral amino acid transporter 1 | SLC38A1 | 54 |
| 0.692 | P08195 | Isoform 2 of 4F2 cell-surface antigen heavy chain | SLC3A2 | 58 |
| 0.702 | Q9H5Q4 | Dimethyladenosine transferase 2, mitochondrial | TFB2M | 45 |
| 0.712 | P29317 | Ephrin type-A receptor 2 | EPHA2 | 108 |
| 0.714 | O14786 | Neuropilin-1 | NRP1 | 101 |
| 0.723 | P11279 | Lysosome-associated membrane glycoprotein 1 | LAMP1 | 39 |
| 0.726 | Q96PD2 | Discoidin, CUB and LCCL domain-containing protein 2 | DCBLD2 | 85 |
| 0.747 | P16070 | CD44 antigen (Fragment) | CD44 | 20 |
| 0.754 | P46734 | Dual specificity mitogen-activated protein kinase kinase 3 | MAP2K3 | 39 |
| 0.765 | P08754 | Guanine nucleotide-binding protein G(k) subunit alpha | GNAI3 | 41 |
| 0.766 | Q9H5V8 | CUB domain-containing protein 1 | CDCP1 | 93 |
| 0.777 | Q13641 | Trophoblast glycoprotein | TPBG | 46 |

Table 1. Cont.

| Ratio ¹ | Protein IDs | Protein Description | Gene Name | MW [kDa] ² |
|--------------------|-------------|---|-----------|-----------------------|
| 0.809 | P02795 | Metallothionein-2 | MT2A | 6 |
| 0.811 | Q14978 | Nucleolar and coiled-body phosphoprotein 1 | NOLC1 | 74 |
| 0.825 | P52926 | High mobility group protein HMGI-C | HMG2A | 11 |
| 0.833 | P08962 | CD63 antigen | CD63 | 16 |
| 0.837 | P32455 | Interferon-induced guanylate-binding protein 1 | GBP1 | 68 |
| 0.837 | P04183 | Thymidine kinase, cytosolic | TK1 | 25 |
| 0.848 | Q16831 | Uridine phosphorylase 1 | UPP1 | 34 |
| 0.858 | P21980 | Protein-glutamine gamma-glutamyltransferase 2 | TGM2 | 69 |
| 0.875 | P35080 | Profilin-2 | PFN2 | 10 |
| 0.882 | P13726 | Tissue factor | F3 | 33 |
| 0.885 | P56945 | Breast cancer anti-estrogen resistance protein 1 | BCAR1 | 93 |
| 0.891 | O15118 | Niemann-Pick C1 protein | NPC1 | 142 |
| 0.892 | Q14669 | E3 ubiquitin-protein ligase TRIP12 | TRIP12 | 220 |
| 0.92 | Q12996 | Cleavage stimulation factor subunit 3 | CSTF3 | 83 |
| 0.935 | Q9H4A6 | Golgi phosphoprotein 3 | GOLPH3 | 34 |
| 0.942 | Q16850 | Isoform 2 of lanosterol 14- α demethylase | CYP51A1 | 46 |
| 0.962 | P11802 | Cyclin-dependent kinase 4 | CDK4 | 34 |
| 0.97 | Q9Y3E0 | Vesicle transport protein GOT1B | GOLT1B | 14 |
| 0.975 | Q9Y3D8 | Transcription initiation factor TFIID subunit 9 | AK6 | 17 |
| 0.983 | Q9UBB6 | Isoform 2 of neurochondrin | NCDN | 77 |
| 1.003 | P17844 | Probable ATP-dependent RNA helicase DDX5 | DDX5 | 107 |
| 1.028 | P05120 | Plasminogen activator inhibitor 2 | SERPINB2 | 47 |
| 1.085 | P11234 | Ras-related protein Ral-B | RALB | 23 |
| 1.127 | Q96QD8 | Sodium-coupled neutral amino acid transporter 2 | SLC38A2 | 56 |
| 1.162 | P52292 | Importin subunit alpha-1 | KPNA2 | 58 |
| 1.539 | P40189 | Interleukin-6 receptor subunit beta | IL6ST | 104 |
| 1.54 | Q06481 | Amyloid-like protein 2 | APLP2 | 76 |
| 1.742 | P05067 | Gamma-secretase C-terminal fragment 59 | APP | 81 |
| 2.309 | P09914 | Interferon-induced protein with tetratricopeptide repeats 1 | IFIT1 | 55 |
| 2.408 | P02787 | Serotransferrin | TF | 78 |
| 2.809 | O60603 | Toll-like receptor 2 | TLR2 | 90 |

¹: LOG (FAC/Veh, 2); ²: MW: relative molecular mass (MW) generated by the MS system.

Table 2. Differentially expressed proteins involved in various iron overload-induced biological process in HH4 cells.

| Biological Process | Related Gene |
|---|---|
| Response to wounding | CD44; F3; DCBLD2; GPX1; MAP2K3; NRP1; SERPINB2; SOD2; THBS1; TLR2; TF; Tfr1 |
| Di-, tri-valent inorganic cation homeostasis | ACO1; APP; APLP2; IL6ST; MT2A; SRI; SOD2; TF; Tfr1; TGM2 |
| Regulation of growth | CD44; AK6; APP; CSF1; CYR61; DCBLD2; HMG2A; IDH3G; NRP1; BCAR1 |
| Positive regulation of signal transduction | F3; CSF1; GPX1; GOLPH3; GOLT1B; IL6ST; THBS1; TGM2 |
| Anti-apoptosis | SH3GLB1; F3; GPX1; SERPINB2; SOD2; THBS1; TGM2 |
| Inflammatory response | CD44; F3; MAP2K3; THBS1; TLR2; TF; Tfr1 |
| Positive regulation of cell migration | F3; CSF1; ICAM1; IL6ST; BCAR1; THBS1 |
| Endocytosis | ATP6V1H; EHD2; NPC1; APP; THBS1; Tfr1 |
| Iron ion homeostasis | ACO1; SRI; SOD2; TF; Tfr1 |
| Response to hypoxia | ALDOC; SOD2; THBS1; TF; Tfr1 |
| Positive regulation of cytokine production | PYCARD; IL6ST; THBS1; TLR2 |
| Apoptotic mitochondrial changes | SH3GLB1; GPX1; SOD2 |
| Positive regulation of NF- κ B transcription factor activity | PYCARD; ICAM1; TLR2 |

2.2. Analysis of Proteomics Data

Next, we analyzed 93 differentially expressed proteins using Ingenuity Pathways Analysis (IPA) (Ingenuity Systems, Redwood, CA, USA, www.ingenuity.com). The metabolic and canonical pathways as well as the interconnecting proteins were generated.

The results showed that 13 proteins were involved in cell-to-cell signaling and interaction, inflammatory response and cellular movement pathway (Figure 2A). Twelve proteins were involved in cellular movement, inflammatory response and immune cell trafficking pathway (Figure 2B). These findings indicate that HH4 cell proteomes were markedly shifting after FAC overload treatment.

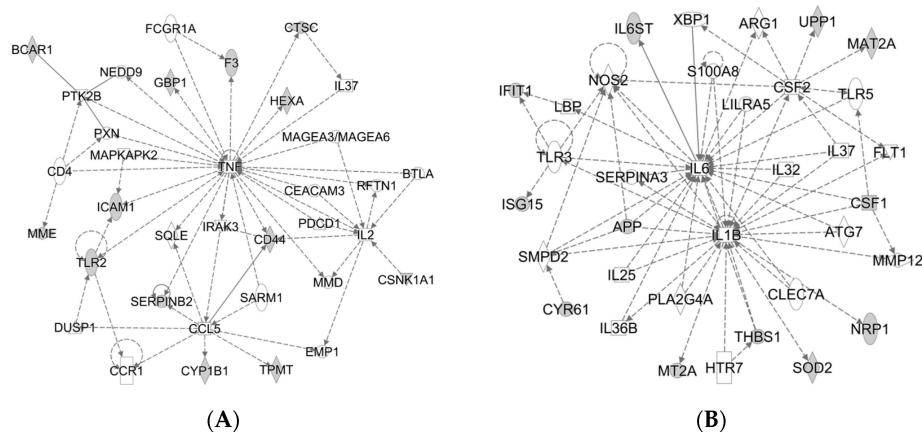


Figure 2. Biological pathways analysis of differentially expressed proteins in HH4 cells. (A) Top network functions of cell-to-cell signaling and interaction, inflammatory response, cellular movement and (B) immune cell trafficking using Ingenuity Pathways Analysis (IPA). Solid lines: direct known interactions. Dashed lines: suspected or indirect interactions. White: proteins known to be in the network but not identified in our study.

2.3. Validation of LC-MS/MS Results by RT-PCR

In order to verify the accuracy of protein identifications made by LC-MS/MS, we randomly selected 11 proteins from 93 differentially expressed proteins to validate their mRNA levels. The results, as shown in Figure 3A, indicate when HH4 cells were treated with 5 mM FAC for 24 h, mRNA levels of gene IL6ST, APP, TF, TLR2, MME, Tfr1 and CHCHD2 increased 1.7, 1.7, 13.6, 4.6, 3.1, 1.7, and 1.9 times, respectively compared to untreated HH4 cells. In addition, as shown in Figure 3B, the mRNA levels of GLG1, THBS1, EHD2 and CYP1B1 reduced 0.7, 0.3, 0.5 and 0.7 times, respectively in FAC-treated cells compared to untreated HH4 cells. Our findings are consistent with the results from proteomic mass spectroscopy.

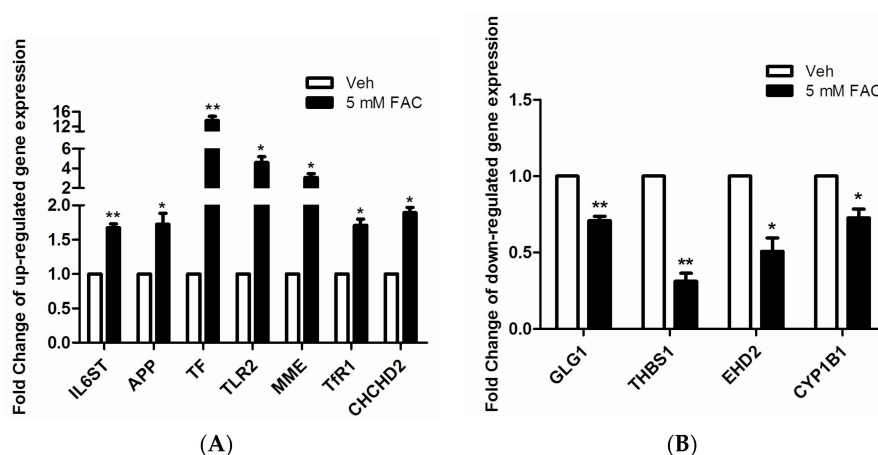


Figure 3. Confirmation of mass spectrometry-determined protein using RT-PCR technique. (A) Gene expression analysis of seven kinds of up-regulated proteins randomly selected from 93 kinds of differentially expressed proteins; (B) Gene expression analysis of four kinds of down-regulated proteins randomly selected from 93 kinds of differentially expressed proteins. The expression of genes was classified as up-regulated if expression levels were >1.5-fold and as down-regulated if levels were <0.67-fold, relative to control HH4 cells. Expression of β -actin was used as internal control. Results are shown as mean \pm SEM of three independent experiments. Statistically significant differences are labeled as * $p < 0.05$ and ** $p < 0.01$, compared with the control groups, using unpaired Student's t test.

2.4. FAC-Induced Iron Overload Affected Iron Homeostasis Related Proteins

After annotated the function of 93 differentially expressed proteins, we found the level of intracellular iron homeostasis related proteins increased significantly in FAC treated HH4 cells, such as IL6ST, TF and Tfr1. It is well known that hepcidin is the center regulator to ensure iron metabolism in steady state. Therefore, we were interested in whether FAC-induced iron overload can affect expression of hepcidin and iron regulatory related proteins. As shown in Figure 4A, mRNA levels of gene Tfr2, IL-6, STAT3, hepcidin and ferritin significantly increased after 24 h of exposure to 5 mM FAC in HH4 cells, suggesting FAC exposure facilitated TF-Tfr2 and IL 6-STAT3 signaling pathway to further activate hepcidin expression (Figure 4B).

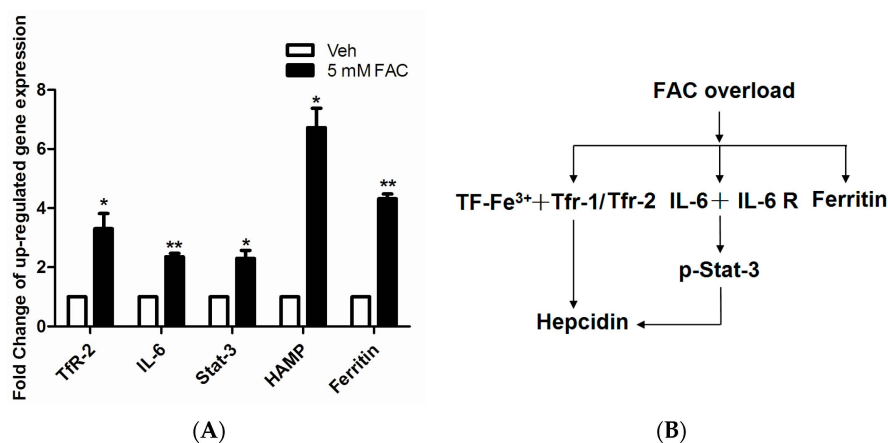


Figure 4. The effect of FAC overload on expression levels of iron homeostasis related gene. **(A)** FAC overload induced upregulation of iron homeostasis related protein expression. Expression of β -actin was used as internal control. Results are shown as mean \pm SEM of three independent experiments. Statistically significant differences are labeled as * $p < 0.05$ and ** $p < 0.01$, compared with the control groups, using unpaired Student's t test; **(B)** Schematic representation of the activation of Hepcidin regulation-associated signal transduction pathway in HH4 cells with FAC treatment.

2.5. FAC Overload Triggered TLR2-Mediated Inflammatory Response

In the foregoing analysis via GO and IPA, we noticed that TLR2 was involved in FAC-induced iron overload in HH4 cells (Figure 1B, Table 2, Figure 2A) and the mRNA level of TLR2 was also consistent with proteomics data (Figure 3A). We next investigated the protein level of TLR2 and its related pathway in FAC treated HH4 cells. As shown in Figure 5A, protein levels of TLR2 significantly increased in HH4 cells after 24 h of exposure to 5 mM FAC and its downstream factor, MyD88, was also significantly increased, indicating that FAC treatment activated the TLR2-MyD88 signaling pathway. In order to clarify the specific role of TLR2 in FAC treated hepatocytes, we next inhibited the endogenous TLR2 expression in HH4 cells using RNA interference.

As shown in Figure 5B, inhibition using siRNA significantly reduced protein levels of TLR2. In addition, inhibition of TLR2 markedly decreased the expression of IL-6 and IL6ST at transcriptional level in FAC-treated HH4 cells, compared to untreated cells (Figure 5C). Our data also indicated p-NF- κ B but not p-p38 involving in activation of TLR2-IL6 pathway (Figure 5C,D). Taken together, these results suggested that TLR2-mediated inflammatory response triggered by FAC induced the expression of IL-6 through activating the NF- κ B pathway rather than p38 pathway in HH4 cells.

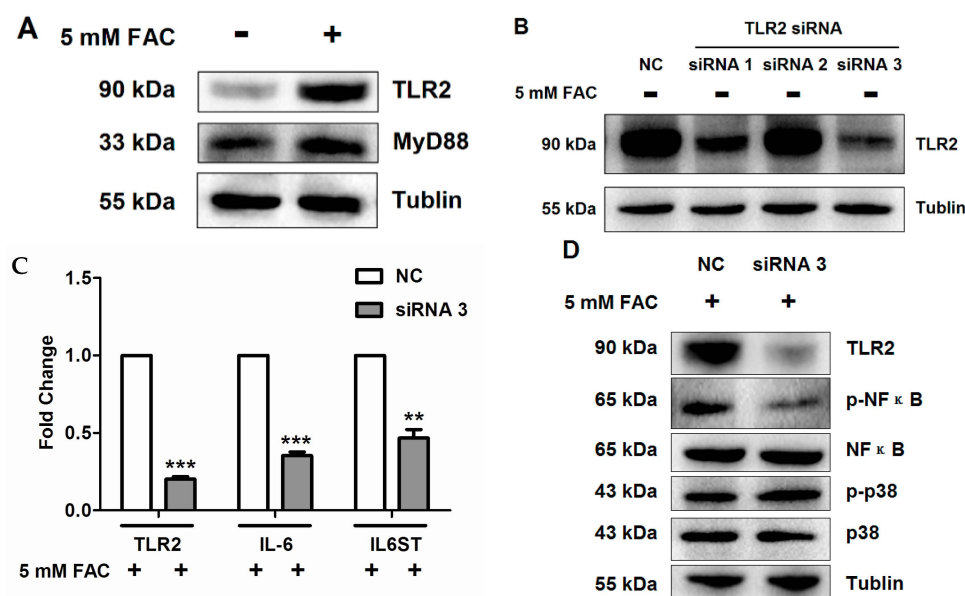


Figure 5. The activation of TLR2 pathway induced by iron overload in HH4 cells. (A) Protein expression of TLR2 and MyD88 were analyzed by western blot in HH4 cells after 24 h of 5 mM FAC treatment; (B) Inhibitory effects of siRNA for TLR2 in HH4 cells. Cells (10^5 cells/well) were pre-treated with 60 nM siRNA for TLR2 for 48 h and then interference efficiency was estimated by detection of protein expression levels of TLR2 using western blot assay. NC = negative control siRNA; siRNA 1 = TLR2 siRNA (950 bp); siRNA 2 = TLR2 siRNA (1377 bp); siRNA 3 = TLR2 siRNA (1648 bp); (C) Effects of siRNA for TLR2 on transcriptional levels of IL-6 and IL6ST in HH4 cells. Cells (10^5 cells/well) were pre-treated with 60 nM siRNA for TLR2 for 48 h. Then HH4 cells were treated with 5 mM FAC for 24 h and transcriptional levels of gene IL-6 and IL6ST via RT-PCR assay. Expression of β -actin was used as internal control. Results are shown as mean \pm SEM of three independent experiments. Statistically significant differences are labeled as ** $p < 0.01$ and *** $p < 0.001$, compared with the control groups, using unpaired Student's *t* test; (D) Effects of siRNA for TLR2 on NF- κ B and p38 pathway in HH4 cells. Cells (10^5 cells/well) were pre-treated with 60 nM siRNA for TLR2 for 48 h. Then HH4 cells were treated with 5 mM FAC for 24 h and the protein expression levels of p-NF- κ B, NF- κ B, p-p38 and p38 using Western blot assay. +: in the presence of 5mM FAC, -: in the absence of 5mM FAC.

3. Discussion

HCT is by far the most effective way to treat the clonal disorder disease [6]. However, patients commonly have an increase of nontransferrin-bound iron (NTBI) and show hepatic iron overload already before HCT or after transplant conditioning [7,8]. Excessive iron can stimulate the formation of ROS via the Fenton reaction [9], and progressive accumulation of ROS may damage mitochondrial and nuclear DNA through lipid peroxidation [10]. In our previous work, we have shown that iron overload can induce apoptosis via both extrinsic and intrinsic pathways in hepatic cells [5]. To our knowledge, the exact cellular consequences and the cellular processes of iron overload in hepatocytes are still not very clear. In this current study, we utilized proteomics technique to dissect more signaling pathways that related to hepatocytes iron overload.

The mass spectrum results showed FAC-induced HH4 cells contained 93 differentially expressed proteins and activated multiple pathways (Figure 1A and Table 1). Levels of protein ATP6V1H, which facilitates acidification of intracellular endosomes formed by transferrin/transferrin receptor-mediated endocytosis [11,12], increased 1.6 times (Table 1), while levels of protein EHD2, which plays an important role in regulating transferrin exit from ERC (endocytic recycling compartment) [13], decreased three times (Table 1) when HH4 cells were treated with 5 mM FAC at 24 h. These two

significantly changed proteins indicate that HH4 cells may absorb a large number of extracellular iron ion via endocytosis.

Addition of excess iron inevitably led to iron dyshomeostasis and thus triggered differential expression of intracellular iron homeostasis associated proteins in HH4 cells (Figure 1B). Levels of protein TF (serotransferrin) which is mainly produced by hepatocytes and capable of binding excess iron ions and delivering it into cells increased sharply in FAC-overload HH4 cells (Table 1 and Figure 3A). Levels of protein IRP1, which is also known as cytoplasmic aconitate hydratase (ACO1), and is the trans-acting factor located in the cytoplasm that can bind with high affinity to RNA motifs related to iron homeostasis [14], decreased 0.5 times (Table 1) and levels of the protein ferritin, each molecule of which is capable of storing up to 4500 iron atoms [15], increased 4.4 times (Figure 4A) in FAC-treated HH4 cells. Meanwhile, our MS data displayed the expression of γ -secretase C-terminal fragment 59 and amyloid-like protein 2 were increased 3.3-fold and 2.9-fold in FAC treated cells, respectively (Table 1), suggesting that full length APP protein, which can stabilize surface FPN, may participate in the efflux of iron from HH4 cells [16]. Our MS data also showed the expression of metallothionein-2 increased 1.8 times but SOD2 expression decreased 0.6 times in iron-loaded HH4 cells. Metallothioneins (MTs), which are conserved in the animal kingdom, can chelate heavy and trace metals such as zinc, copper or iron through sulfur-based clusters, and therefore the main function of MTs is the regulation of homeostasis, like the protection against oxidative stress or metals [17]. While SOD2 (superoxide dismutase [Mn], mitochondrial) functioned as the antioxidant is known to scavenge the ROS, specifically the hydroxyl radical [18]. In a word, these significantly changed proteins indicate that iron overload induces biological process of di-, tri-valent inorganic cation homeostasis in HH4 cells (Figure 1B and Table 2).

In addition, hepcidin is undoubtedly the most central regulator of iron hemostasis, and our results also confirmed that FAC-induced HH4 cells showed evidently enhanced transcription levels of gene TF, Tfr1/2, IL-6, IL6ST, STAT3 and hepcidin (Figure 4), indicating that hepcidin was involved in the re-regulation of iron homeostasis in iron overload-treated HH4 cells.

Mass spectral analysis also indicated the participation of other biological process including response to wounding, cell apoptosis and inflammatory response in FAC-induced HH4 cells. For example, thrombospondin-1 (THBS1) which is a matricellular glycoprotein first discovered in activated platelets that plays an important role in the process of wound healing [19], decreased 0.47 times (Table 1 and Figure 3B), while the expression of endophilin-B1, which is involved in the regulation of apoptosis helping the maintenance of mitochondrial morphology and autophagy [20], was apparently increased in HH4 cells after iron overload treatment (Table 1). Among these, the most interestingly finding is the expression of inflammation mediator TLR2 increased markedly in FAC-treated HH4 cells (Table 1). Inflammation is a fundamental biological process that stands at the foreground of acute and chronic pathological conditions [21]. Toll-like receptors (TLRs) discovered in the 1990s are a family of very similar proteins containing leucine-rich repeats and their activation triggers a signaling cascade which leads to the production of cytokines/chemokines, further initiating an inflammatory response [22]. So far 13 TLRs have been identified, 10 human TLRs (TLR1-10), and 12 mouse TLRs (TLR1-9, TLR11 and TLR12) [23]. It is well known that the acute phase response to infection and inflammation can cause alterations in iron homeostasis, thereby reducing iron supplies to pathogens. A recent study found that the acute inflammatory condition mediated by TLR2 and TLR6 induced rapid hepcidin-independent hypoferremia through decreasing the messenger RNA and protein expression of ferroportin (FPN) in mice injected with TLR ligands [24]. Although TLR2 has been implicated in the response to infection mediated by TLR2 ligands, includes molecules with diacyl and triacylglycerol moieties, proteins and polysaccharides, scanty data is available on the direct relationship between TLR2 and iron overload. Therefore, our next research validated TLR2 mRNA and protein expression in FAC treated HH4 cells (Table 1, Figures 3A and 5A), which is consistent with proteomics data. In addition, our experiment indicated that inhibition of TLR2 by siRNA inactivated IL-6 expression via NF- κ B pathway in FAC treated hepatocytes (Figure 5).

4. Experimental Section

4.1. Cell Culture

The non-transformed human hepatocyte cell line HH4 was maintained as described previously [7]. Briefly, HH4 cells were maintained in Williams' medium E (Gibco Laboratories, Grand Island, NY, USA), supplemented with 10% fetal bovine serum (FBS), 0.1% ITS, dexamethasone (0.04 µg/mL) (Sigma Chemical Co., St. Louis, MO, USA), gentamycin (50 µg/mL) (Sigma Chemical Co.), HEPES (20 mM) and sodium pyruvate (1 mM) (Gibco Laboratories).

4.2. In Vitro Iron Overload Model

The *in vitro* iron overload model was established as previously described [5]. Briefly, HH4 cells were seeded in 15 cm culture dishes at 1×10^5 cells/mL, incubated overnight at 37 °C in 5% CO₂ atmosphere, and then treated with or without 5 mM FAC (Sigma Chemical Co.) for 24 h. The experiments were repeated three times.

4.3. Proteomics Analysis

4.3.1. Cell Lysis and Protein Digestion

HH4 cells were washed three times with PBS buffer, harvested by trypsinization, and centrifuged at $1000 \times g$ for 5 min. After the addition of T-PER Reagent (Thermo Scientific, Rockford, CA, USA), PMSF (1 mM) and 0.1% aprotinin, the cell pellets were lysed for 30 min on ice and centrifuged at $13,800 \times g$ for 15 min. Then the supernatant was transferred into new tubes. The Bradford assay was used to determine the protein concentration (Beyotime Institute of Biotechnology, Shanghai, China). Proteins were reduced with 10 mM dithiothreitol (DTT) at 56 °C for 45 min and then alkylated with 10 mM iodoacetamide (IAM) (Sigma Chemical Co.) for 20 min at room temperature in the dark. The sample was diluted four times with 40 mM ammonium bicarbonate buffer. Sequencing grade trypsin (Promega, Madison, WI, USA) was added in a 1:50 (*w/w*) ratio and the incubation was carried out overnight at 37 °C. After an over-night digestion peptides were recovered from the filter. Peptides were desalted with Oasis 1cc cartridges and flow through from Oasis cartridge was desalted with Sep-Pak C18 1cc (Waters, Milford, MA, USA). Elutions from Oasis and Sep-Pak were combined together and concentrated in SpeedVac.

4.3.2. Nanoflow LC-MS/MS

Peptide digests dissolved in loading buffer (0.1% trifluoroacetic acid—TFA) were loaded onto an in-house packed 20 cm capillary column with 3 µm Reprosil-Pur C18 beads (Dr. Maisch GmbH, Ammerbuch, Germany) using an EASY-nLC 1000 system (Thermo Scientific). Running buffer A was 0.1% TFA in water and running buffer B was 0.1% TFA in ACN (acetonitrile). The total gradient was 120 min and the flow rate started at 300 nL/min. The detailed gradient was 6% ACN with a linear increase to 30% ACN over 105 min followed by 4 min linear increase to 90% ACN. MS data were acquired using a data-dependent top-20 method on Q Exactive (Thermo Scientific, Bremen, Germany). Spray voltage was set to 2.0 kV, S-lens RF level at 60, and capillary temperature at 275 °C. Full scan resolutions were set to 60,000 at *m/z* 200 and AGC (automatic gain control) was 3×10^6 with a maximum fill time of 20 ms. The range of full mass was set to 350–1500 *m/z*. MS2 scan resolutions were set to 15,000 at *m/z* 200 and AGC was 5×10^4 with a maximum fill time of 45 ms. Isolation width was set at 1.6 Th. A fixed first mass of 110 was used. Normalized collision energy was set at 27. Peptide match was set to “preferred” and isotope exclusion was on. Precursor ions with single, un-assigned, charge states were removed from fragmentation selection [25–27].

4.3.3. Data Analysis

All data were analyzed with the MaxQuant version 1.5.1.12 [28], with the Andromeda search engine [29]. The false discovery rate (FDR) was set at 1% for protein, peptide spectrum match. Peptides were required to have a minimum length of six amino acids and a maximum mass of 10,000 Da. Fragmentation spectra were searched by Andromeda in the Uniprot human database (version 201502; 90,300 entries) combined with 262 common contaminants [29]. Enzyme specificity was set as C-terminal to arginine and lysine and a maximum of two missed cleavages. Second peptides search was enabled. For proteome identification, carbamidomethylation (C) was set as a fixed modification. deamidation (NQ) and oxidation (M) were set as variable modifications. To identify significantly regulated proteins, LFQ intensities were used. Proteins with p -value < 0.05, fold change > 1.5 or < 0.67 were recognized as significant change.

4.4. Realtime-PCR

Total RNA was extracted using RNA pure Tissue Kit (Cwbio, Beijing, China) according to the manufacturer's instruction. Real-time RT-PCR amplification was performed using an Ultra SYBR mixture kit (Cwbio) on the C1000 Touch Thermal Cycler (Bio-Rad, Hercules, CA, USA), and the results were analyzed using CFX Manager software (Bio-Rad). Target gene expression levels were quantified using the formula $2^{-\Delta\Delta Ct}$ method [30]. Primer sequences (Invitrogen Corporation, Shanghai, China) and optimal PCR annealing temperatures are listed in Table 3.

Table 3. Forward and reverse primer sequences, annealing temperature and product size for different genes.

| Gene | Primer | Sequence (5'-3') | Product Size (bp) | Annealing Temperature (°C) |
|----------------|---------|--------------------------|-------------------|----------------------------|
| IL6ST | Forward | GTGAGTGGGATGGTGGAAAGG | 78 | 60 |
| | Reverse | CAAACCTGTGTGTGCCCATTC | | |
| APP | Forward | GCCCTGCGGAATTGACAAG | 144 | 60 |
| | Reverse | CCATCTGCATAGTCTGTGTCTG | | |
| TF | Forward | GGTGGCAGAGTTCATGGGTC | 172 | 60 |
| | Reverse | ACAGTAAAGTAAGCCTATGGGGA | | |
| TLR2 | Forward | ATCCTCCAATCAGGCTTCTCT | 118 | 60 |
| | Reverse | GGACAGGTCAAGGCTTTTACA | | |
| MME | Forward | GATCGCACTCTATGCAACCTAC | 83 | 60 |
| | Reverse | TGTTTTGGATCAGTCGAGCAG | | |
| TfR1 | Forward | ACCATTGTTCATATACCCGGTTCA | 219 | 60 |
| | Reverse | CAATAGCCCAAGTAGCCAATCAT | | |
| CHCHD2 | Forward | ACACATTGGGTCACGCCATTA | 201 | 60 |
| | Reverse | GCACCTCATTGAAACCCTCACA | | |
| GLG1 | Forward | CCAAGATGACGGCCATCATT | 103 | 60 |
| | Reverse | AGCCGAATACTGCCACATTC | | |
| THBS1 | Forward | TGCTATCACAACGGAGTTCAGT | 108 | 60 |
| | Reverse | GCAGGACACCTTTTTGCAGATG | | |
| EHD2 | Forward | TCCGCAAACCTCAACCCTTTC | 78 | 60 |
| | Reverse | TCTCCAGGACCTGATTAGGGA | | |
| CYP1B1 | Forward | ACGTACCGGCCACTATCACT | 142 | 60 |
| | Reverse | CTCCCCACGACCTGATCCA | | |
| TfR2 | Forward | AATGTCCTGAGTCAGAGCGG | 141 | 55.9 |
| | Reverse | GGCAGACTCTACTGGAGCGA | | |
| IL6 | Forward | CCAGAGCTGTGCAGATGAGT | 99 | 57.8 |
| | Reverse | CATTTGTGGTTGGGTCAGG | | |
| STAT3 | Forward | ACACACGGTACCTGGAGCAG | 172 | 57.8 |
| | Reverse | TACTGCTGGTCAATCTCTCCC | | |
| Ferritin | Forward | ATCAACCTGGAGCTCTACGC | 155 | 57.8 |
| | Reverse | TGGTTCTGCAGCTTCATCAG | | |
| HAMP | Forward | CTGTTTTCCACAACAGAC | 230 | 59.8 |
| | Reverse | CCTTCCTTATTTATTCCTGC | | |
| β -actin | Forward | CTCCTGGGCATGGAGTC | 232 | 60 |
| | Reverse | GCCGATCCACACGGAGTA | | |

4.5. Western Blot Analysis

Cells were lysed with RIPA (1% Triton X-100, 150 mM NaCl, 25 mM Tris pH 7.4, 5 mM EDTA, 0.5% sodium deoxycholate, 0.1% SDS, 5 mM tetrasodium pyrophosphate, 50 mM sodium fluoride, 1 mM Na₃VO₄, 2 mM phenylmethanesulfonyl fluoride, 0.076 U/mL aprotinin). After centrifugation at 13,800 × g for 15 min, the supernatants were collected. Protein content was determined using BCA Protein Assay. Equal amounts of protein were subjected to SDS-PAGE. Proteins were electrophoretically transferred to PVDF membranes (Bio-Rad), and blocked with phosphate buffered saline/0.05% Tween-20 (PBS-T) containing 5% non-fat dry milk or BSA at room temperature (RT) for 1 h. Membranes were incubated with primary antibody TLR2, MyD88 (Abcam, Cambridge, MA, USA), p-p38 MAPK, p38 MAPK, p-NF-κB or NF-κB (Cell Signaling Technology, Boston, MA, USA) at a 1:1000 dilution in PBS-T at 4 °C overnight, washed four times with PBS-T, and then incubated with horseradish peroxidase (HRP)-conjugated secondary antibody (Beyotime Institute of Biotechnology) in PBS-T at room temperature for 1 h. Protein was detected using an enhanced chemoluminescence (ECL) kit (Tiangen, Beijing, China).

4.6. RNA Interference (RNAi) of Gene TLR2

For gene silencing assays, the small interfering RNA of TLR2 (siTLR2) gene and negative control siRNA (siNC) were synthesized by Invitrogen Corporation. The sense and anti-sense strands of siRNAs were: siRNA 1, 5'-GGUGAAACAAUUC AUUGATT-3' (sense), 5'-UCAAUGAAU UUGUUUCACCTT-3' (antisense); siRNA 2, 5'-CCUCUCUACAAACUUUAAUTT-3' (sense), 5'-AUUAAAGUUUGUAGAGAGGTT-3' (antisense); siRNA 3, 5'-GCAACUCAAGAACUUU AU TT-3' (sense), 5'-AUAAGUUUCUUUGAGUUGCTT-3' (antisense); hepatocytes were transiently transfected with oligofectamine according to the manufacturer's protocol in the presence or absence of 60 nM siRNA duplex. Western blot analysis of protein expression level of TLR2 was performed to identify inhibitory effect of siRNA in HH4 cell. After 48 h transfection with indicated siRNA, cells were treated with 5 mM FAC for 24 h and then the expression of a series of inflammation-related genes was detected using quantitative real-time RT-PCR or Western blot assay.

4.7. Statistical Analysis

Results were analyzed by one-way analysis of variance (ANOVA) or 2-sample unpaired *t*-test using Prism 5 program (Version 5.0). Differences in results were considered significant when *p* values were ≤ 0.05. Results are given as mean ± SEM of at least 3 independent experiments.

5. Conclusions

This is the first global proteomic analysis that compares the protein signatures of FAC-exposed HH4 cells with normal HH4 cells. Our study results suggest differentially expressed proteins are involved in multiple biological process including endocytosis, di-, tri-valent inorganic cation homeostasis, response to wounding, inflammatory response, anti-apoptosis, apoptotic mitochondrial changes and other processes. In addition, this work suggests for the first time that FAC overload can induce TLR2-mediated acute inflammatory response and activate IL6 expression via NF-κB pathways in HH4 cells. Our results should provide a theoretical basis for drug therapy of iron-associated liver damage.

Acknowledgments: This work was supported by grants from the National Science Foundation of China (Grant No. 81470294 and 31400691), the Natural Science Foundation of Jiangsu Province (Grant No. BK20140169), and the Fundamental Research Funds for the Central Universities (Grant No. JUSRP51619B).

Author Contributions: Xiang Li, Shiwei Li and Xin Zhou designed research; Shiwei Li, Mize Lu, Guohua Yang and Yunfeng Shen performed research and analyzed the data; Shiwei Li and Xiang Li wrote the paper. All authors read and approved the final manuscript.

Conflicts of Interest: There is no conflict of interest.

References

1. Armand, P.; Kim, H.T.; Cutler, C.S.; Ho, V.T.; Koreth, J.; Alyea, E.P.; Soiffer, R.J.; Antin, J.H. Prognostic impact of elevated pretransplantation serum ferritin in patients undergoing myeloablative stem cell transplantation. *Blood* **2007**, *109*, 4586–4588. [[CrossRef](#)] [[PubMed](#)]
2. Locasciulli, A.; Oneto, R.; Bacigalupo, A.; Socié, G.; Korthof, E.; Bekassy, A.; Schrezenmeier, H.; Passweg, J.; Führer, M. Outcome of patients with acquired aplastic anemia given first line bone marrow transplantation or immunosuppressive treatment in the last decade: A report from the European Group for Blood and Marrow Transplantation. *Haematologica* **2007**, *9*, 11–18. [[CrossRef](#)]
3. Platzbecker, U.; Bornhäuser, M.; Germing, U.; Stumpf, J.; Scott, B.L.; Kröger, N.; Schwerdtfeger, R.; Böhm, A.; Kobbe, G.; Theuser, C. Red blood cell transfusion dependence and outcome after allogeneic peripheral blood stem cell transplantation in patients with de novo myelodysplastic syndrome (MDS). *Biol. Blood Marrow Transplant.* **2008**, *14*, 1217–1225. [[CrossRef](#)] [[PubMed](#)]
4. Zhao, M.; Laissue, J.A.; Zimmermann, A. Hepatocyte apoptosis in hepatic iron overload diseases. *Histol. Histopathol.* **1997**, *12*, 367–374. [[PubMed](#)]
5. Li, S.W.; Liu, C.M.; Guo, J.; Marcondes, A.M.; Deeg, J.; Li, X.; Guan, F. Iron overload induced by ferric ammonium citrate triggers reactive oxygen species-mediated apoptosis via both extrinsic and intrinsic pathways in human hepatic cells. *Hum. Exp. Toxicol.* **2015**. [[CrossRef](#)] [[PubMed](#)]
6. Laport, G.G.; Sandmaier, B.M.; Storer, B.E.; Scott, B.L.; Stuart, M.J.; Lange, T.; Maris, M.B.; Agura, E.D.; Chauncey, T.R.; Wong, R.M. Reduced-intensity conditioning followed by allogeneic hematopoietic cell transplantation for adult patients with myelodysplastic syndrome and myeloproliferative disorders. *Biol. Blood Marrow Transplant.* **2008**, *14*, 246–255. [[CrossRef](#)] [[PubMed](#)]
7. Li, X.; Xu, F.; Karopongse, E.; Marcondes, A.M.; Lee, K.; Kowdley, K.V.; Miao, C.H.; Trobridge, G.D.; Campbell, J.S.; Deeg, H.J. Allogeneic transplantation, Fas signaling, and dysregulation of hepcidin. *Biol Blood Marrow Transplant.* **2013**, *19*, 1210–1219. [[CrossRef](#)] [[PubMed](#)]
8. Sahlstedt, L.; Ebeling, F.; Von Bonsdorff, L.; Parkkinen, J.; Ruutu, T. Non-transferrin-bound iron during allogeneic stem cell transplantation. *Brit. J. Haematol.* **2001**, *113*, 836–838. [[CrossRef](#)]
9. Galaris, D.; Pantopoulos, K. Oxidative stress and iron homeostasis: mechanistic and health aspects. *Crit. Rev. Clin. Lab. Sci.* **2008**, *45*, 1–23. [[CrossRef](#)] [[PubMed](#)]
10. Yakes, F.M.; Van Houten, B. Mitochondrial DNA damage is more extensive and persists longer than nuclear DNA damage in human cells following oxidative stress. *Proc. Natl. Acad. Sci. USA* **1997**, *94*, 514–519. [[CrossRef](#)] [[PubMed](#)]
11. Andrews, N.C. Forging a field: The golden age of iron biology. *Blood* **2008**, *112*, 219–230. [[CrossRef](#)] [[PubMed](#)]
12. Molina, M.F.; Qu, H.-Q.; Rentfro, A.R.; Nair, S.; Lu, Y.; Hanis, C.L.; McCormick, J.B.; Fisher-Hoch, S.P. Decreased expression of ATP6V1H in type 2 diabetes: A pilot report on the diabetes risk study in Mexican Americans. *Biochem. Biophys. Res. Commun.* **2011**, *412*, 728–731. [[CrossRef](#)] [[PubMed](#)]
13. George, M.; Ying, G.G.; Rainey, M.A.; Solomon, A.; Parikh, P.T.; Gao, Q.; Band, V.; Band, H. Shared as well as distinct roles of EHD proteins revealed by biochemical and functional comparisons in mammalian cells and *C. elegans*. *BMC Cell Biol.* **2007**, *8*, 3. [[CrossRef](#)] [[PubMed](#)]
14. Meyron-Holtz, E.G.; Ghosh, M.C.; Rouault, T.A. Mammalian tissue oxygen levels modulate iron-regulatory protein activities *in vivo*. *Science* **2004**, *306*, 2087–2090. [[CrossRef](#)] [[PubMed](#)]
15. Fleming, R.E.; Ponka, P. Iron overload in human disease. *N. Engl. J. Med.* **2012**, *366*, 348–359. [[CrossRef](#)] [[PubMed](#)]
16. Wong, B.X.; Tsatsanis, A.; Lim, L.Q.; Adlard, P.A.; Bush, A.I.; Duce, J.A. β -Amyloid precursor protein does not possess ferroxidase activity but does stabilize the cell surface ferrous iron exporter ferroportin. *PLoS ONE* **2014**, *9*, e114174. [[CrossRef](#)] [[PubMed](#)]
17. Schuermann, A.; Helker, C.S.M.; Herzog, W. Metallothionein 2 regulates endothelial cell migration through transcriptional regulation of vegfc expression. *Angiogenesis* **2015**, *18*, 463–475. [[CrossRef](#)] [[PubMed](#)]
18. Puukila, S.; Bryan, S.; Laakso, A.; Abdel-Malak, J.; Gurney, C.; Agostino, A.; Belló-Klein, A.; Prasad, K.; Khaper, N. Secoisolaricresinol diglucoside abrogates oxidative stress-induced damage in cardiac iron overload condition. *PLoS ONE* **2015**, *10*, e0122852. [[CrossRef](#)] [[PubMed](#)]
19. Agah, A.; Kyriakides, T.R.; Lawler, J.; Bornstein, P. The lack of thrombospondin-1 (TSP1) dictates the course of wound healing in double-TSP1/TSP2-null mice. *Am. J. Pathol.* **2002**, *161*, 831–839. [[CrossRef](#)]

20. Karbowski, M.; Jeong, S.-Y.; Youle, R.J. Endophilin B1 is required for the maintenance of mitochondrial morphology. *J. Cell. Biol.* **2004**, *166*, 1027–1039. [[CrossRef](#)] [[PubMed](#)]
21. Lugin, J.; Rosenblatt-Velin, N.; Parapanov, R.; Liaudet, L. The role of oxidative stress during inflammatory processes. *Biol. Chem.* **2014**, *395*, 203–230. [[CrossRef](#)] [[PubMed](#)]
22. Rajamani, U.; Jialal, I. Hyperglycemia induces Toll-like receptor-2 and -4 expression and activity in human microvascular retinal endothelial cells: implications for diabetic retinopathy. *J. Diabetes Res.* **2014**, *2014*, 790902. [[CrossRef](#)] [[PubMed](#)]
23. Oliveira-Nascimento, L.; Massari, P.; Wetzler, L.M. The role of TLR2 in infection and immunity. *Front. Immunol.* **2012**, *3*. [[CrossRef](#)] [[PubMed](#)]
24. Guida, C.; Altamura, S.; Klein, F.A.; Galy, B.; Boutros, M.; Ulmer, A.J.; Hentze, M.W.; Muckenthaler, M.U. A novel inflammatory pathway mediating rapid hepcidin-independent hypoferremia. *Blood* **2015**, *12*, 2265–2275. [[CrossRef](#)] [[PubMed](#)]
25. Kelstrup, C.D.; Jersie-Christensen, R.R.; Batth, T.S.; Arrey, T.N.; Kuehn, A.; Kellmann, M.; Olsen, J.V. Rapid and deep proteomes by faster sequencing on a benchtop quadrupole ultra-high-field Orbitrap mass spectrometer. *J. Proteome Res.* **2014**, *13*, 6187–6195. [[CrossRef](#)] [[PubMed](#)]
26. Kelstrup, C.D.; Young, C.; Lavalley, R.; Nielsen, M.L.; Olsen, J.V. Optimized fast and sensitive acquisition methods for shotgun proteomics on a quadrupole orbitrap mass spectrometer. *J. Proteome Res.* **2012**, *11*, 3487–3497. [[CrossRef](#)] [[PubMed](#)]
27. Scheltema, R.A.; Hauschild, J.P.; Lange, O.; Hornburg, D.; Denisov, E.; Damoc, E.; Kuehn, A.; Makarov, A.; Mann, M. The Q Exactive HF, a Benchtop mass spectrometer with a pre-filter, high-performance quadrupole and an ultra-high-field Orbitrap analyzer. *Mol. Cell. Proteom.* **2014**, *13*, 3698–3708. [[CrossRef](#)] [[PubMed](#)]
28. Cox, J.; Mann, M. MaxQuant enables high peptide identification rates, individualized p.p.b.-range mass accuracies and proteome-wide protein quantification. *Nat. Biotechnol.* **2008**, *26*, 1367–1372. [[CrossRef](#)] [[PubMed](#)]
29. Cox, J.; Neuhauser, N.; Michalski, A.; Scheltema, R.A.; Olsen, J.V.; Mann, M. Andromeda: A peptide search engine integrated into the MaxQuant environment. *J. Proteome Res.* **2011**, *10*, 1794–1805. [[CrossRef](#)] [[PubMed](#)]
30. Livak, K.J.; Schmittgen, T.D. Analysis of relative gene expression data using real-time quantitative PCR and the $2^{-\Delta\Delta CT}$ method. *Methods* **2001**, *25*, 402–408. [[CrossRef](#)] [[PubMed](#)]

Sample Availability: Not Applicable.



© 2016 by the authors; licensee MDPI, Basel, Switzerland. This article is an open access article distributed under the terms and conditions of the Creative Commons by Attribution (CC-BY) license (<http://creativecommons.org/licenses/by/4.0/>).